Elastoplastic Stress–Strain Analysis for a Pure Bending Notched Specimen of Power Hardening Material and its Application

MA WEIDIAN*, HOU CHUNXIAO**, XU XIANG XING**
ZHOU WEI***, SU YI** and CAI QIGONG**

*China Software Technique Corporation, Beijing, PRC
**Department of Mechanical Engineering, Tsinghua University, Beijing, PRC
***University of Cambridge, Cambridge, UK

ABSTRACT

Using the finite element method, an elastoplastic stress–strain analysis for a V-notched specimen in plane-strain pure bending has been carried out. Assuming that the stress-strain relation obeys Ramberg-Osgood law, the contribution of hardening exponent n to stress intensification R (the ratio of the peak value of the maximum principal stress to yield stress, σ_{1max}/σ_0) has been investigated. The variations of R with the hardening exponent and load ratio L/L_{GY} (or σ_{nom}/σ_0) are graphically reported. Based on the results of the analysis, the cleavage fracture stress σ_f' of a power hardening material has been determined.

KEYWORDS

Stress intensification; notched specimen; FEM analysis; power hardening; cleavage fracture stress.

INTRODUCTION

A pure bending V-notched specimen is often used in cleavage fracture research. To investigate the fracture micromechanism and establish the fracture criterion, one should first have a knowledge of the stress distribution in the specimen (Liu and Cai, 1981; Hou, 1985). Until recently, the finite element solution for the stress-strain distributions for a linear hardening material by Griffiths and Owen (1971) have often been referred to. But most of engineering steels are of power hardening characteristics, and their stress-strain relations usually can be approximated by Ramberg-Osgood formula. Different kind of steel exhibits different hardening exponent. Even for the same steel, hardening exponent changes as the temperature varies. Therefore it is necessary to carry out an elastoplastic finite element analysis for the pure bending V-notched specimen at different hardening exponents.

DESCRIPTION OF THE FINITE ELEMENT METHOD

The computer program is developed by Ma *et al.* (1987) for the elastoplastic FEM analysis of V-notched and cracked specimens. The incremental self modifying chord stiffness method (Ma, 1987), which is far more precise than the incremental finite element methods currently used, is employed in the analysis. The finite element mesh is composed of 480 nodes and 866 triangular elements, which is shown in Fig.1. The dimension, load and reaction (shown in Fig.1) conform to Griffiths and Owen's (1971).

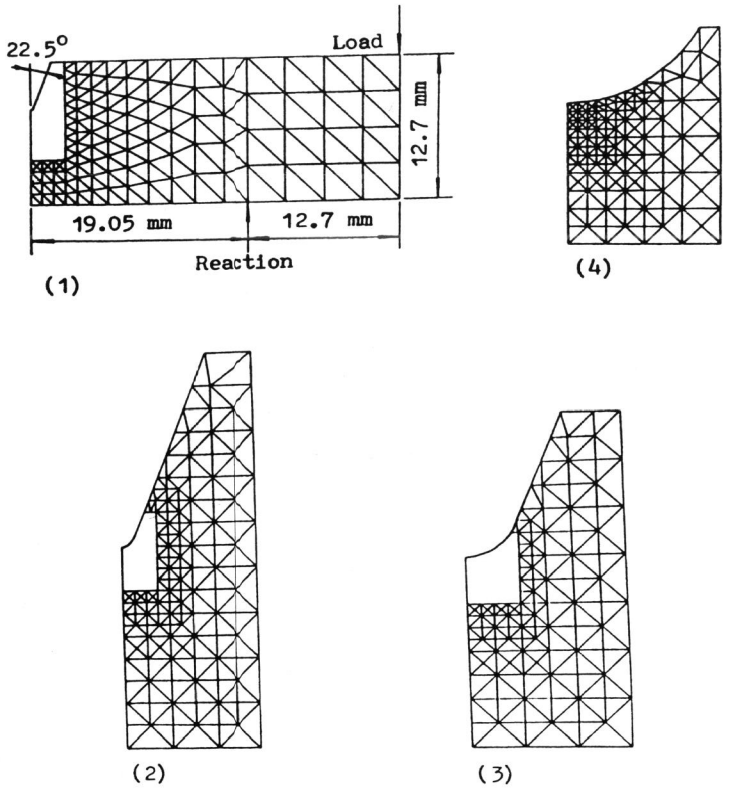

Fig.1. Notch-bend specimen and finite element mesh. Notch root radius ρ=0.25 mm; Specimen thickness B=12.7 mm.

Assume that the materials obey the Ramberg-Osgood constitutional equation

$$\epsilon/\epsilon_0 = \sigma/\sigma_0 + \alpha(\sigma/\sigma_0)^{1/n} \qquad (1)$$

where $\epsilon_0=\sigma_0/E$, uniaxial yield stress σ_0=666.4 MPa, α=0.60024, Poisson's ratio ν =0.28 and Young's modulus E=2×10^5 MPa. The hardening exponents n=0.10, 0.12, 0.14, 0.16, ..., 0.28 and 0.30. The analysis is carried out under the plane strain condition.

As have been done by Griffiths and Owen (1971), the load is expressed by load ratio σ_{nom}/σ_0 or L/L_{GY}. σ_{nom} is the nominal bending stress, i.e.

$$\sigma_{nom} = 6M/Ba^2 \qquad (2)$$

where M is the applied bending couple, and B the specimen thickness. a=8.47mm, is the specimen depth below the notch. L is the load, L_{GY} the general yield load (Griffiths and Owen, 1971). The relation between σ_{nom}/σ_0 and L/L_{GY} is

$$\sigma_{nom}/\sigma_0 = 2.15L/L_{GY} \qquad (3)$$

The stresses are divided the yield stress to give dimensionless forms, e.g., the maximum principal stress is expressed by σ_1/σ_0. Effective strain ϵ_{eff} is obtained using

$$\epsilon_{eff} = \frac{2}{3}\sqrt{\epsilon_x^2+\epsilon_y^2-\epsilon_x\epsilon_y+\frac{3}{4}\gamma_{xy}} \qquad (4)$$

The distance below the notch root, x, is normalized as x/ρ, where ρ is the notch root radius.

To investigate the reliability of the computer program, first the program was run to analyse the strain and stress field in a centre-cracked plate, with the ratio of crack length to plate width, a/b=1/5, and the constitutional equation being

$$\epsilon/0.003332 = \sigma/666.4 + 0.60024(\sigma/666.4)^5 \qquad (5)$$

Based on the obtained stress and strain fields, the J-integral has been evaluated. A comparison was made between the so obtained J-integral values at different nominal tensile stress levels and those obtained by EPRI method (Kumar *et al.*, 1981), which is shown in Table 1. It can be seen from Table 1 that the program is highly reliable. After the reliability investigation, the program was formally run to analyse the stress and strain distributions in the notched specimen.

Table 1 Comparison of J_{FEM} with J_{EPRI}

	0.016	0.232	0.507	0.590	0.739	0.802	0.909	1.230
J_{FEM}/J_{EPRI}	0.950	0.952	0.997	1.019	1.027	1.037	1.035	1.002

In the analysis, the number of load increment steps, N, is 39 for every hardening exponent n. Fig.2 shows the variation of the stress intensification R with the load ratio σ_{nom}/σ_0 (or L/L_{GY}) for n=0.2 with N=10, 19, and 39 individually. It demonstrates that the results are consistent with each other at different steps 10, 19 and 39, therefore the load increment is small enough to get the convergent results when N=39.

The number of the elements in the mesh is larger than that used by Griffiths and Owen (1971), and the element density transition is more reasonable. Unlike the Griffiths and Owen's (1971) mesh, the one used in present study does not contain obtuse triangular elements which will lower the precision of the analysis. With the more precise elastoplastic finite element analysis method, the high reliability of the program, and reasonably small load increment, the more precise results can be expected.

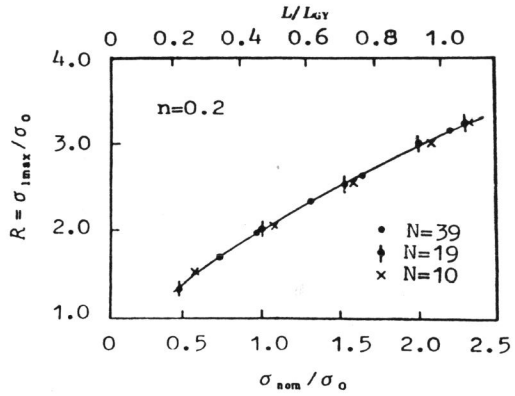

Fig.2. Stress intensification vs. applied load, computed by taking different steps of load increments.

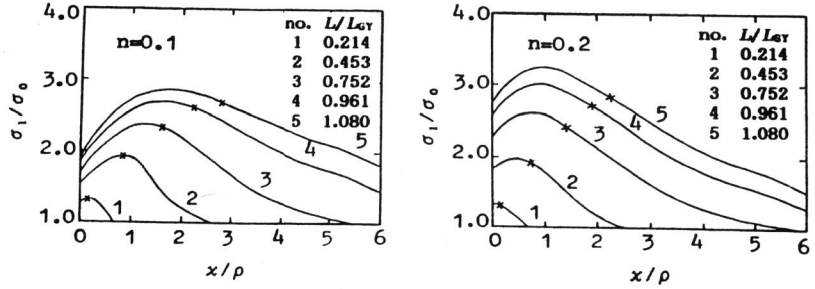

Fig.3. Variation of maximum principal stress below notch root at various loads. x marks plastic-elastic interface.

RESULTS OF THE ANALYSIS

It is indicated by the analysis that the peak value of the maximum principal stress occurs at some distance away from the notch root. The distributions of the maximum principal stress σ_1 below the notch root at various loads, with hardening exponents n=0.10 and 0.20 are shown in Fig.3. It can be seen that when n is constant, the larger the load, the further the location of the peak value of σ_1 gets apart both from the notch root and the elastic-plastic interface, and that when load remains the same, the larger the hardening exponent, the larger σ_{1max}, and the nearer the location of σ_{1max} to the notch root.

The ratio of the peak value of the maximum principal stress to the

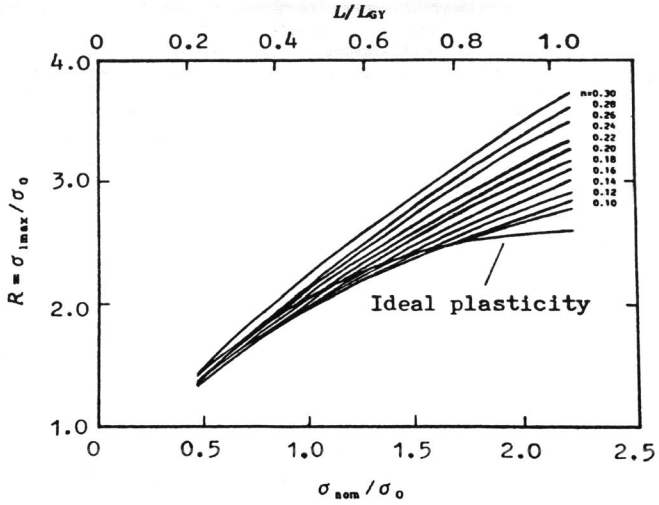

Fig.4. Variation of stress intensification with applied load.

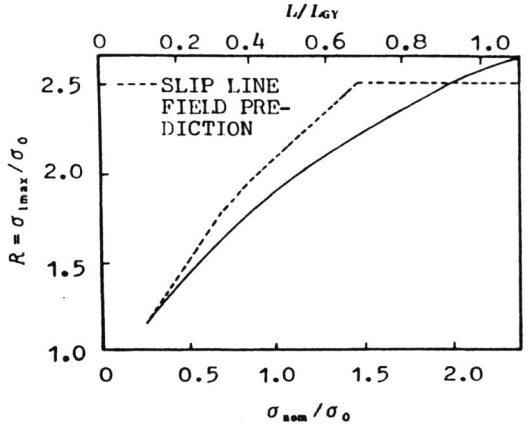

Fig.5. Variation of stress intensification with applied load (Griffiths and Owen, 1971).

yield stress σ_{1max}/σ_0 is defined as stress intensification R. The R curves against load at different hardening exponents are shown in Fig.4. To compare with current results, the R curve obtained by Griffiths and Owen is also presented (Fig.5). There are obvious differences among the R curves at different n under the same load, and the larger the n, the greater the R.

When load gets bigger, the differences become larger. There are also evident differences between the results from power hardening FEM solution and that from linear hardening solution (Griffiths and Owen, 1971). The differences vary with n. For example, at the load level σ_{nom}/σ_0=1.763 (or L/L_{GY} =0.82), when n=0.10, the relative error is 12%; when n=0.20, it is 32%; and when n=0.30, it is 63%. Therefore for power hardening materials, it will introduce a large error when using the Griffiths and Owen's solution.

The distributions of the effective strain ϵ_{eff} below the notch root at various loads are shown in Fig.6 for n=0.1 and 0.2. After data regression, the effective strain has been brought into a uniform analytical expression:

$$\epsilon_{eff} = \epsilon_r \cdot \exp(-1.52x/\rho) \qquad (5)$$

where ϵ_r is the effective strain at the notch root.

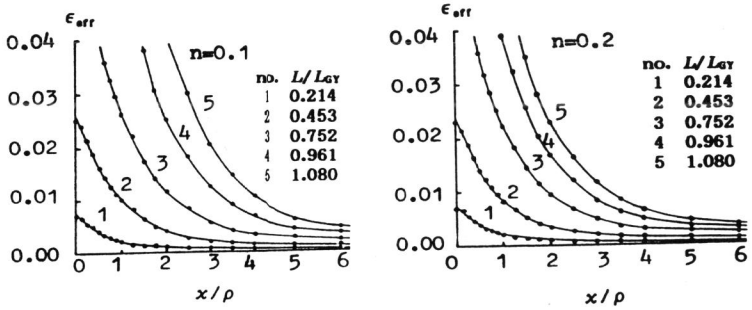

Fig.6. Effective strain below notch root at various loads.

AN EXAMPLE IN PRACTICAL USE

Determination of the cleavage fracture stress using the stress intensification curves in Fig.4 is one of the practical uses for the results of the FEM analysis. By means of thermal simulation, weld heat affected zone (HAZ) in 15MnVN steel has been obtained. The steel is first heated to 1195°C, then sustained for 6 seconds above 1100°C, and after that air cooled. The cooling time from 800°C to 500°C are 77 seconds. The thermally simulated microstructure is shown in Fig.7.

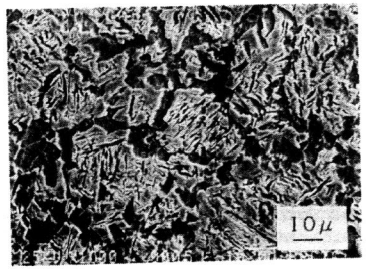

Fig.7. Thermally simulated microstructure of HAZ in 15MnVN steel.

The relation between the hardening exponent n and temperature obtained by Hou *et al.* (1986) was employed in the present study:

T(K)	288	272	258	228	213	193	173	77
n	0.10	0.10	0.11	0.12	0.12	0.13	0.14	0.10

The simulated material is trimmed into the notched specimens as shown in Fig.1. The specimens are loaded at low shelf temperatures to ensure cleavage fracture and the fracture loads are recorded. The stress intensification R at the fracture load is obtained using Fig.4. And the cleavage fracture stress σ_f^* at the temperature is got through $\sigma_f^* = R\sigma_0$. Thus obtained variation of the cleavage fracture stress of 15MnVN steel weld heat affect zone with the temperature T is shown in Fig.8. For purpose of comparison, the σ_f^*-T curve based on Griffiths and Owen's linear hardening FEM analysis is also shown in the figure. It can be seen that the σ_f^* based on Griffiths and Owen's analysis is smaller in the experimental temperature range. In the present study, the hardening exponent only varies from 0.10 to 0.14. Within this range, the difference between the stress intensification from present FEM analysis and that from Griffiths and Owen's is not very large, but beyond the range greater difference can be expected.

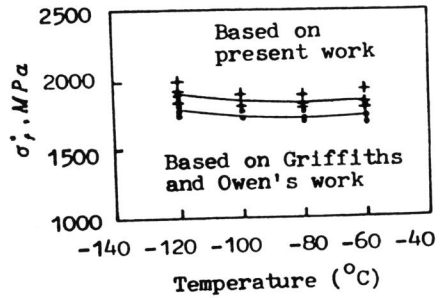

Fig.8. Variation of cleavage fracture stress with temperature.

CONCLUSIONS

Using the elastoplastic FEM program developed by Ma *et al.* (1987), an analysis of the notch root stress and strain distributions in power hardening materials has been carried out. Following are the obtained results:

1. Under the same load, the larger the hardening exponent n, the greater the peak value of the maximum principal stress, and the nearer the position where σ_{1max} occurs to the notch root.

2. For different hardening exponents n, there are large differences among the curves of the stress intensification R versus load ratio σ_{nom}/σ_0 (or L/L_{GY}). As the load ratio gets bigger, the effect of the hardening exponent becomes larger.

3. Generally, the difference between the stress intensification in power hardening materials and that in linear hardening material (Griffiths and Owen, 1971) becomes larger as n increases.

4. The analytical expression for the effective strain below the notch root is presented.

5. Using the stress intensification curves for power hardening materials, the variation of the cleavage fracture stress σ_f^* with the temperature T of the weld heat affected zone in 15MnVN steel has been determined.

REFERENCES

Liu Zuen, Qigong Cai (1985), *Physical Testing and Chemical Analysis (Physical Testing)*, 17, No.5, 19–22.

Hou Chunxiao (1985), *Doctoral Dissertation*, Tsinghua University, Beijing.

Hou Chunxiao, Qigong Cai, Yi Su, Xiuyuan Zhen (1986), *Acta Metall. Sinica*, 22, A506–A514.

Griffiths, J. R. and D. R. J. Owen (1971), *J. Mech. Phys. Solids*, 19, 419–431.

Ma Weidian, Shicheng Chang, Xitang Tian (1987), *Mechanical Strength*, 9, No.4, 62–65.

Kumar, V., M. D. Germen and C. F. Shih (1981), *Topical Report*, No.EPRI-1931, Research Project 1237-1, General Electric Company, Schenectady, NY.